Electronic Supplementary Information

Understanding the correlation and balance between miscibility and optoelectronic properties for polymer-fullerene solar cells

Chaohong Zhang[a] *, Stefan Langner[a], Alexander V. Mumyatov[b], Denis V. Anokhin[b,c,d], Jie Min[e,a], José Darío Perea[a], Kirill L. Gerasimov[d], Andres Osvet[a], Dimitri A. Ivanov [c,d,f], Pavel Troshin[g,b],* Ning Li[a],* and Christoph J. Brabec[a,h]*

[a] Institute of Materials for Electronics and Energy Technology (i-MEET), Friedrich-Alexander University Erlangen-Nürnberg, Martensstrasse 7, 91058 Erlangen, Germany
[b] Institute for Problems of Chemical Physics of Russian Academy of Sciences, Semenov Prospect 1, Chernogolovka, 142432, Russia.
[c] Moscow Institute of Physics and Technology (State University), Institutskiy per. 9, Dolgoprudny, 141700, Russia
[d] Moscow State University, Faculty of Fundamental Physical and Chemical Engineering, GSP-1, 1-51 Leninskie Gory, Moscow, 119991, Russia
[e] The Institute for Advanced Studies, Wuhan University, Wuhan 430072, China
[f] Institut de Sciences des Matériaux de Mullhouse, CNRS UMR 7361, 15 Jean Starcky, F-68051 Mulhouse, France
[g] Skolkovo Institute of Science and Technology, Skolkovo Innovation Center, Nobel st. 3, Moscow, 143026, Russian Federation
[h] Bavarian Center for Applied Energy Research (ZAE Bayern), Haberstrasse 2a, 91058 Erlangen, Germany
* Author to whom correspondence should be addressed. E-mail: chaohong.zhang@fau.de; ning.li@fau.de; christoph.brabec@fau.de; p.troshin@skoltech.ru

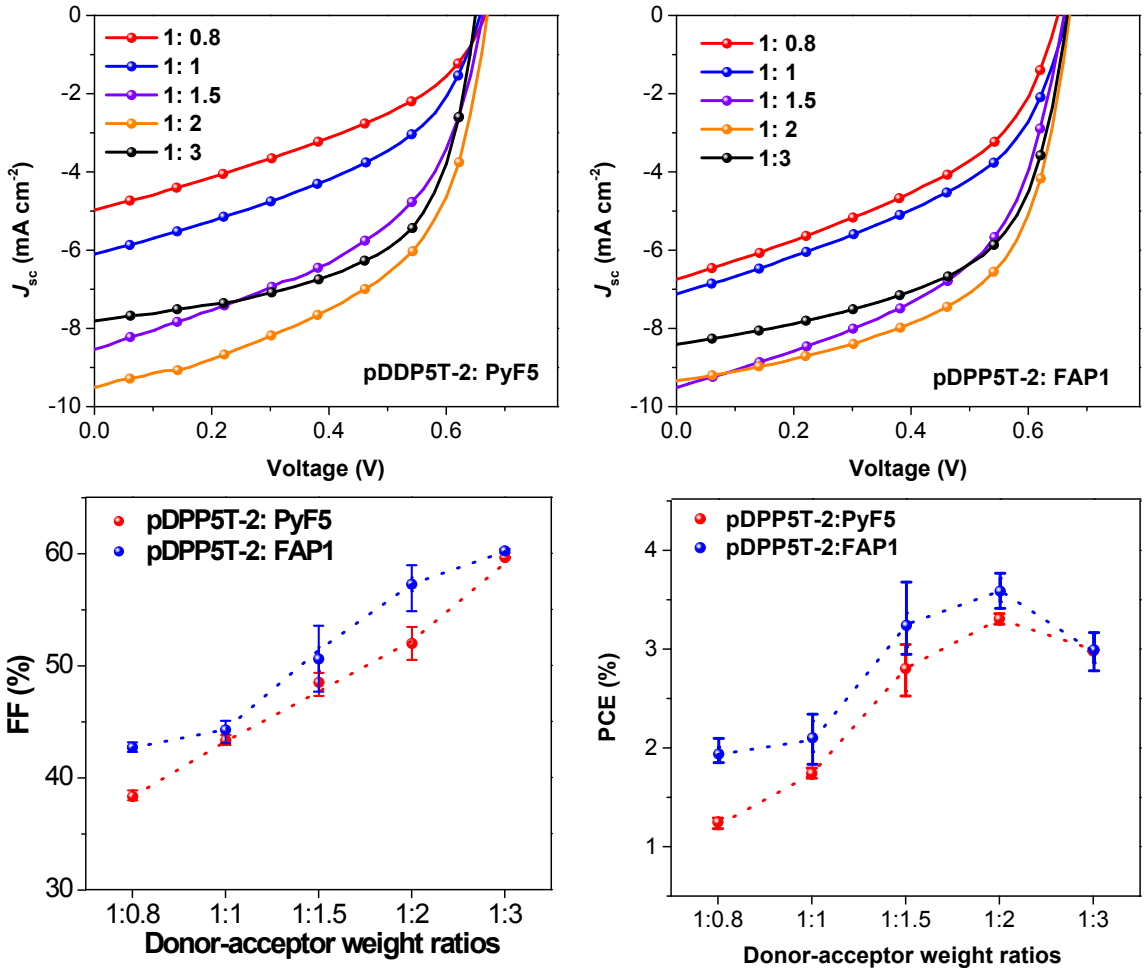

Figure S1. a) Current density-voltage (*J-V*) curves of pDPP5T-2:PyF5 and pDPP5T-2:FAP1; PCE (b) and FF (c) as a function of D:A ratios;

Table S1. Photovoltaic properties of pDPP5T-2 : fullerenes organic solar cells

Active layer	Weight ratios	V_{OC} [V]	J_{SC} [mA/cm^2]	FF [%]	PCE [%]
pDPP5T-2 : PyF 5	1:0.8	0.67±0.01	4.9±0.1	38±0.5	1.2±0.1
	1:1	0.66±0.01	6.1±0.1	43±0.5	1.7±0.1
	1:1.5	0.66±0.01	8.5±0.5	48±2.0	2.7±0.2
	1:2	0.67±0.01	9.5±0.4	52±1.4	3.3±0.1
	1:3	0.65±0.01	7.8±0.3	60±0.6	3.0±0.1
pDPP5T-2 : FAP1	1:0.8	0.65±0.01	6.8±0.5	43±2.1	1.9±0.1
	1:1	0.66±0.01	7.1±0.5	44±0.7	2.1±0.2
	1:1.5	0.67±0.01	9.5±0.3	51±2.0	3.2±0.3
	1:2	0.67±0.01	9.3±0.4	57±1.5	3.6±0.1

	1:3	0.66±0.01	8.4±0.1	60±0.2	3.4±0.2

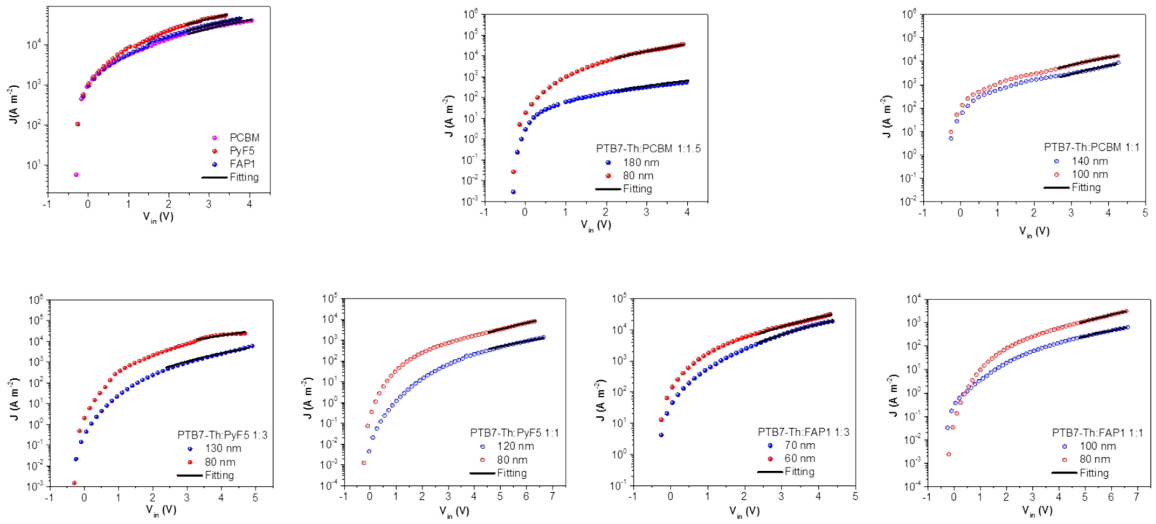

Figure S2. The dark J-V characteristics of (a) PCBM, PyF5 and FAP1 pristine electron-only devices and (b-g) PTB7-Th: fullerenes electron-only devices. The solid line represent the best fitting using the space-charge-limited current (SCLC) modified Mott-Gurney model.

Table S2. Electron mobilities of pristine fullerenes and PTB7-Th: fullerene composites determined from SCLC measurements

Materials	Weight ratios	Electron mobility [$cm^2 V^{-1} s^{-1}$]
PTB7-Th:PCBM	0:1	4.5×10^{-3}
	1:1.5	9.0×10^{-5}
	1:1	9.8×10^{-5}
PTB7-Th : PyF5	0:1	4.0×10^{-3}
	1:3	8.8×10^{-5}
	1:1	8.5×10^{-7}
PTB7-Th : FAP1	0:1	4.4×10^{-3}
	1:3	9.3×10^{-5}
	1:1	4.4×10^{-7}

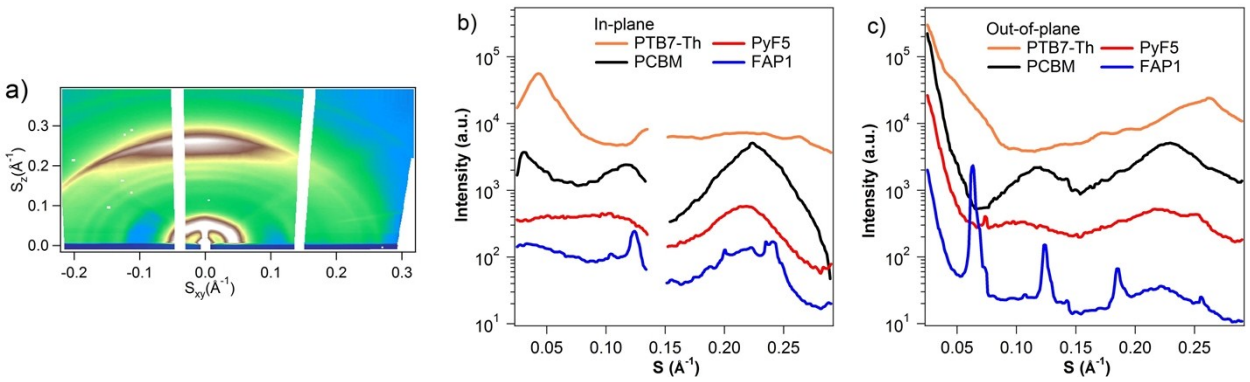

Figure S3. (a) 2D GIWAXS patterns of PTB7-Th; in-plane (b) and Out-of-plane (c) cuts of pristine PTB7-Th, PCBM, PyF5 and FAP1 films.

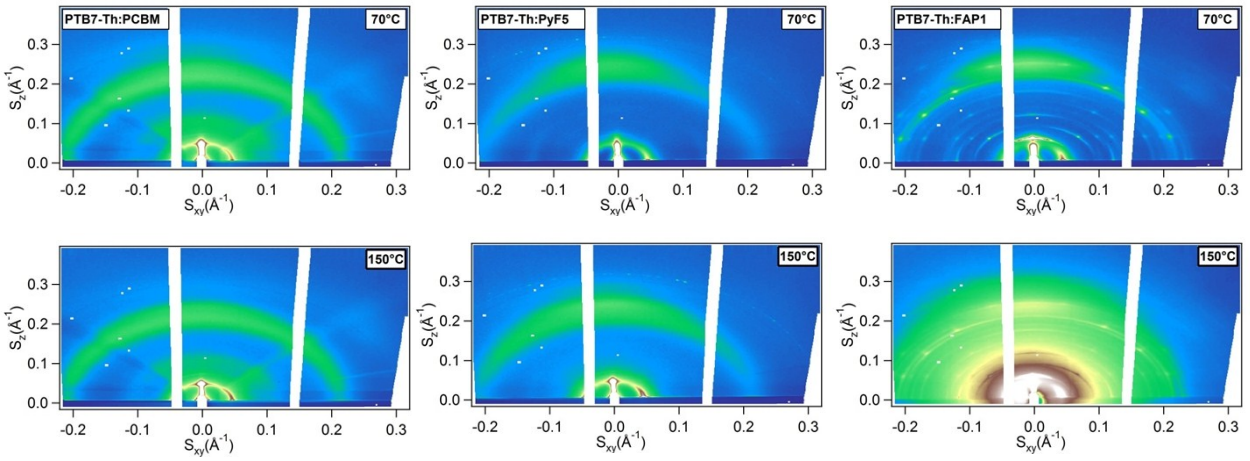

Figure S4. 2D patterns of GIWAXS of PTB7-Th:PCBM, PTB7-Th:PyF5 and PTB7-Th:FAP1 blends at 70 °C and 150 °C.

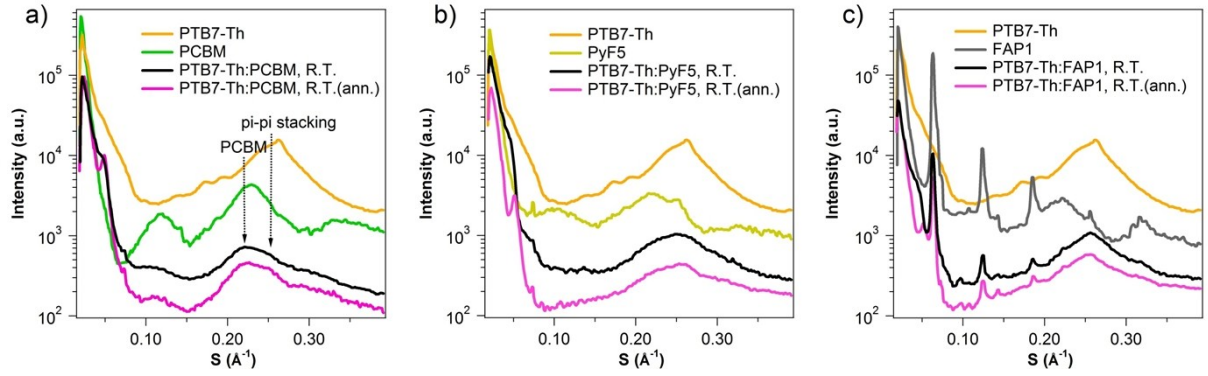

Figure S5. 1D GIWAXS patterns of measured out-of-plane for pure donor and acceptor components and their 1:1 blend before and after annealing: a) PTB7-Th:PCBM;b) PTB7-Th:PyF5; c) PTB7-Th:FAP1.

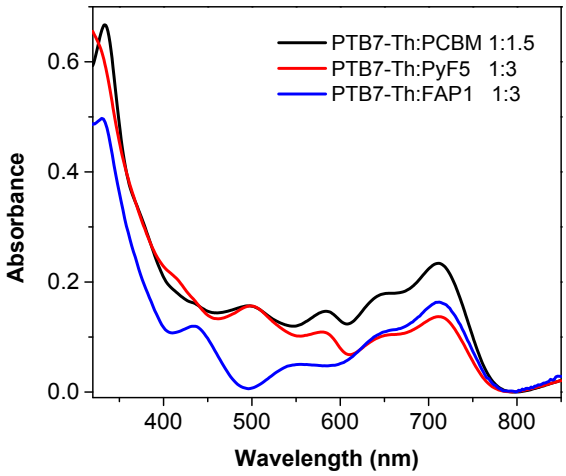

Figure S6. Absorption spectra of ~80 nm thick PTB7-Th:PCBM (1:1.5), PTB7-Th:PyF5 (1:3) and PTB7-Th:FAP1(1:3) thin films.

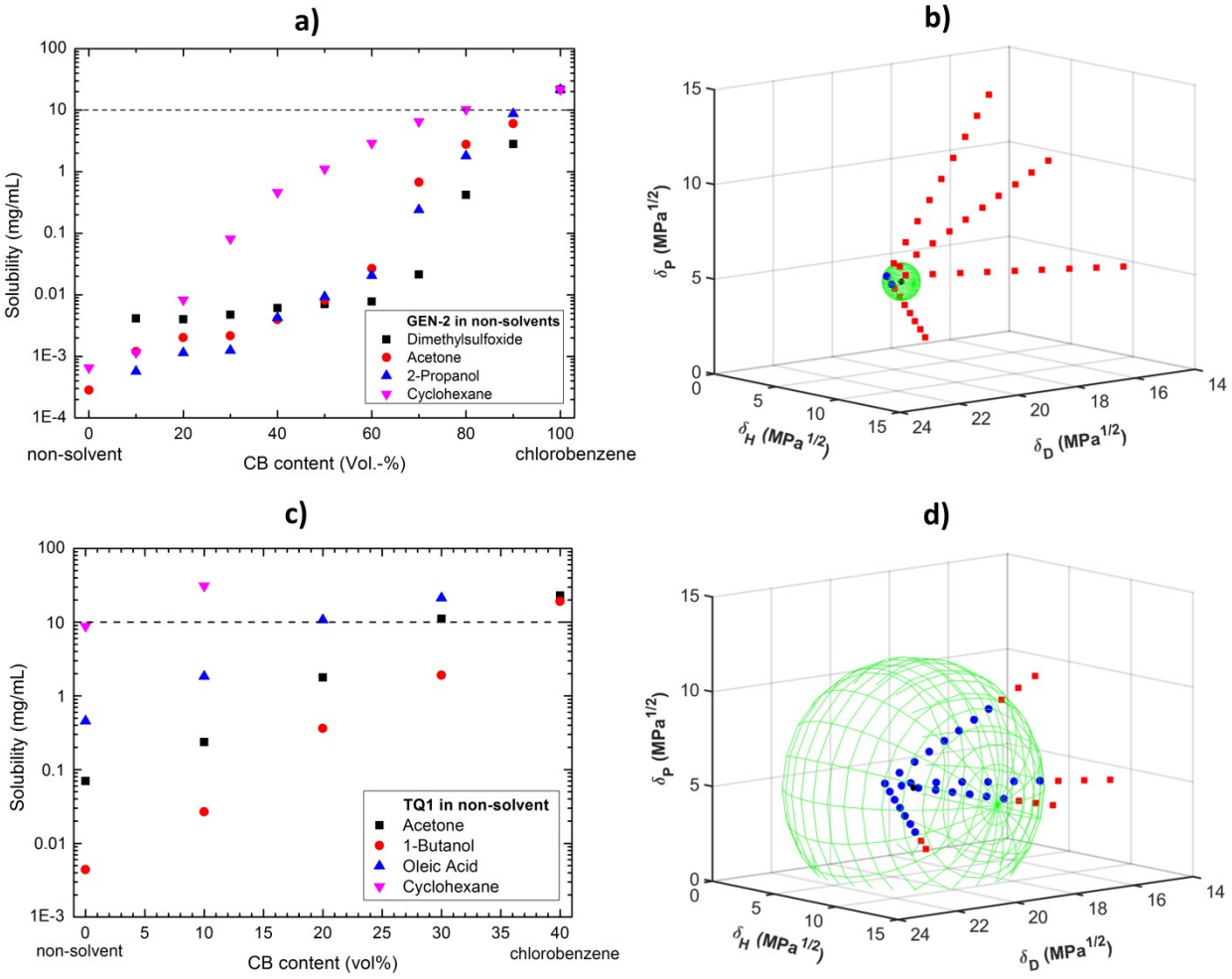

Figure S7. (a) and (c): Solubility of GEN-2 and TQ1 in mixed solvents using chlorobenzene as the good solvent; (b) and (d): Hansen Space and a sphere-fit matching the solubility limit of 10 mg mL^{-1} of GEN-2 and TQ1.

Table S3. Hansen solubility parameters (δ_d, δ_p, and δ_{hb}) and Hildebrand solubility parameter (δ_T) of representative polymers and fullerenes

Materials	δ_d (MPa$^{1/2}$)	δ_p (MPa$^{1/2}$)	δ_{hb} (MPa$^{1/2}$)	δ_T (MPa$^{1/2}$)[a)]	References
PCPDTBT	19.60	3.60	8.80	21.78	[1]
MDMO-PPV	19.06	5.62	5.28	20.56	[2]
MEH-PPV	19.06	5.38	5.44	20.53	[2]
TQ1	19.20	4.50	4.80	20.30	b)
pDPP5T-2	19.00	3.00	2.00	19.30	[3]
GEN-2	18.50	3.90	3.10	19.16	b)
PffBT4T-2OD	18.56	4.07	2.31	19.14	[4]
P3HT	18.50	4.60	1.40	19.11	[5]
PTB7-Th	18.56	2.30	3.21	18.98	[6]
PCBM	20.6	4.93	4.23	21.60	[7]
$PC_{71}BM$	20.95	2.80	1.64	21.20	[7]
PyF5	20.92	2.15	0.19	21.03	[6]
FAP1	20.75	2.60	0.33	20.91	[6]

a) $\delta_T = \sqrt[2]{\delta_d^2 + \delta_p^2 + \delta_{hb}^2}$

b) The Hansen solubility parameters (δ_d, δ_p, and δ_{hb}) of GEN-2 and TQ1 were determined via the binary solvent gradient method, which was employed to probe the surface of the Hansen sphere for a set of four different solvent mixtures.[5, 8] First the solubility of each polymer was measured stepwise from good solvent to non-solvent. Therefore, chlorobenzene was employed as good solvent, while acetone, propylene carbonate, 2-propanol and cyclohexane were used as non-solvents (low solubility of the polymers). Because of different weak forces of the non-solvents (propylene carbonate highly polar or cyclohexane less polar), blends with altered interaction relative to the solute are created. This results in a controlled change in solubility (**Figure S7**). Next, the Hansen solubility parameters of each solvent blend were calculated by following equation:

$$HSP_{blend} = \phi_{S_1} \cdot HSP_{S_1} + \phi_{S_2} \cdot HSP_{S_2} \quad \text{(S1.1)}$$

with ϕ_{S1} and ϕ_{S2} as the volume fraction of chlorobenzene and non-solvent, respectively. This allows us to transfer the solubility data into HSP data, which are then plotted in the Hansen-space. By using a solubility limit of 10 mg mL^{-1}, a 0-1 scoring of the HSP data was made, whereby blend with higher solubility were marked as 1, otherwise 0. Finally a sphere fit was performed by

the software HSPiP. The program evaluates the input data using a quality-of-fit function with the form:

$$DATAFIT = (A_1 A_2 \cdots A_2)^{1/n} \tag{S1.2}$$

With n as the number of solvents and

$$A_i = e^{-(error\ distance)_i} \tag{S1.3}$$

where the error distance is the distance of the solvent in error to the sphere boundary. [5]

The center of the sphere represents then the Hansen solubility parameters of the polymers.

Table S4. Interaction parameters of polymer:fullerenes and the corresponding Acceptor:Donor ratios from literatures

Polymer:fullerene	x_{12}/v_0	$(\delta_1 - \delta_2)^2$	**Optimized devices**	
	(10^{-3}· cm^{-3} · mol)	**(MPa)**	**A:D ratio**	**References**
PCPDTBT:PCBM	0.014	0.034	3.6:1	[9]
MDMO-PPV:PCBM	0.44	1.08	4:1	[10]
MEH-PPV:PCBM	0.45	1.13	5:1	[11]
TQ1:PCBM	0.69	1.70	3:1	[12]
pDPP5T-2:PCBM	2.06	5.11	2:1	[13]
GEN-2:PCBM	2.40	5.96	1.5:1	[14]
PffBT4T-2OD:PCBM	2.44	6.05	1.2:1	[15]
P3HT:PCBM	2.49	6.18	1:1	[16]
PTB7-Th:PCBM	2.78	6.89	1.5:1	this work
PCPDTBT:$PC_{71}BM$	0.14	0.34	3:1	[18]
MDMO-PPV:$PC_{71}BM$	0.16	0.41	4:1	[10]
TQ1:$PC_{71}BM$	0.33	0.82	3:1	[12]
pDPP5T-2:$PC_{71}BM$	1.40	3.46	2:1	[13]
PffBT4T-2OD:$PC_{71}BM$	1.71	4.24	1.2:1	[15]
P3HT:$PC_{71}BM$	1.75	4.35	1:1	[16]
PTB7-Th:$PC_{71}BM$	2.00	4.95	1.5:1	[17]
pDPP5T-2: FAP1	0.98	2.44	2:1	this work
PTB7-Th: FAP1	1.49	3.70	2:1	this work
pDPP5T-2: PyF5	1.11	2.76	2:1	this work
PTB7-Th: PyF5	1.65	4.10	2:1	this work

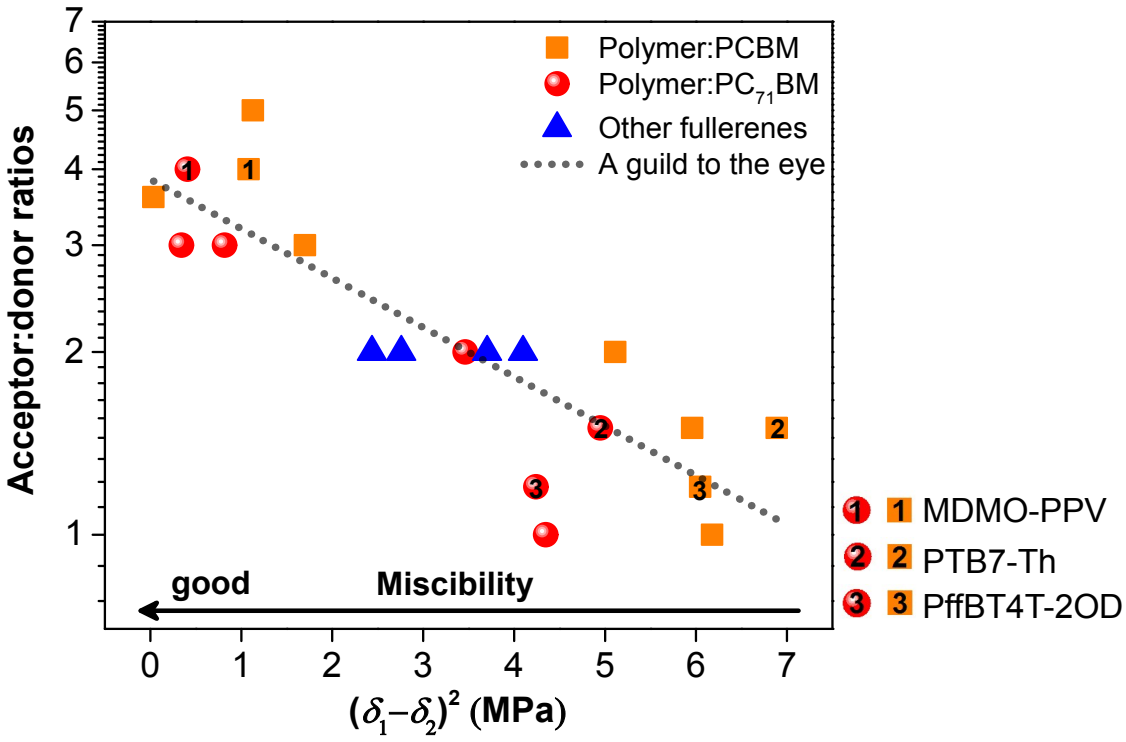

Figure S8. Fullerene acceptor: polymer donor ratios as a function of polymer-fullerene miscibility

References

1. F. Machui, S. Abbott, D. Waller, M. Koppe and C. J. Brabec, *Macromolecular chemistry and Physics*, 2011, **212**, 2159-2165.
2. D. T. Duong, B. Walker, J. Lin, C. Kim, J. Love, B. Purushothaman, J. E. Anthony and T. Q. Nguyen, *Journal of Polymer Science Part B: Polymer Physics*, 2012, **50**, 1405-1413.
3. J. G. Tait, T. Merckx, W. Li, C. Wong, R. Gehlhaar, D. Cheyns, M. Turbiez and P. Heremans, *Advanced Functional Materials*, 2015, **25**, 3393-3398.
4. N. Li, J. D. Perea, T. Kassar, M. Richter, T. Heumueller, G. J. Matt, Y. Hou, N. S. Güldal, H. Chen and S. Chen, *Nature Communications*, 2017, **8**.
5. F. Machui, S. Langner, X. Zhu, S. Abbott and C. J. Brabec, *Solar Energy Materials and Solar Cells*, 2012, **100**, 138-146.
6. C. Zhang, A. Mumyatov, S. Langner, J. D. Perea, T. Kassar, J. Min, L. Ke, H. Chen, K. L. Gerasimov and D. V. Anokhin, *Advanced Energy Materials*, 2016.
7. J. D. Perea, S. Langner, M. Salvador, J. Kontos, G. Jarvas, F. Winkler, F. Machui, A. Görling, A. Dallos, T. Ameri and C. J. Brabec, *The Journal of Physical Chemistry B*, 2016, **120**, 4431-4438.
8. I. Burgués-Ceballos, F. Machui, J. Min, T. Ameri, M. M. Voigt, Y. N. Luponosov, S. A. Ponomarenko, P. D. Lacharmoise, M. Campoy-Quiles and C. J. Brabec, *Advanced Functional Materials*, 2014, **24**, 1449-1457.

9. J. Y. Kim, K. Lee, N. E. Coates, D. Moses, T.-Q. Nguyen, M. Dante and A. J. Heeger, *Science*, 2007, **317**, 222-225.
10. S. E. Shaheen, C. J. Brabec, N. S. Sariciftci, F. Padinger, T. Fromherz and J. C. Hummelen, *Applied Physics Letters*, 2001, **78**, 841-843.
11. S. Alem, R. de Bettignies, J.-M. Nunzi and M. Cariou, *Applied physics letters*, 2004, **84**, 2178-2180.
12. E. Wang, L. Hou, Z. Wang, S. Hellström, F. Zhang, O. Inganäs and M. R. Andersson, *Advanced Materials*, 2010, **22**, 5240-5244.
13. V. S. Gevaerts, A. Furlan, M. M. Wienk, M. Turbiez and R. A. Janssen, *Advanced Materials*, 2012, **24**, 2130-2134.
14. N. Li, D. Baran, K. Forberich, F. Machui, T. Ameri, M. Turbiez, M. Carrasco-Orozco, M. Drees, A. Facchetti and F. C. Krebs, *Energy & Environmental Science*, 2013, **6**, 3407-3413.
15. Y. Liu, J. Zhao, Z. Li, C. Mu, W. Ma, H. Hu, K. Jiang, H. Lin, H. Ade and H. Yan, *Nat Commun*, 2014, **5**, 5293.
16. M. T. Dang, L. Hirsch and G. Wantz, *Advanced Materials*, 2011, **23**, 3597-3602.
17. Z. He, B. Xiao, F. Liu, H. Wu, Y. Yang, S. Xiao, C. Wang, T. P. Russell and Y. Cao, *Nature Photonics*, 2015, **9**, 174-179.
18. M. M. Wienk, J. M. Kroon, W. J. Verhees, J. Knol, J. C. Hummelen, P. A. van Hal and R. A. Janssen, *Angewandte Chemie*, 2003, **115**, 3493-3497.